Chemistry & Biology
Brief Communication

Superagonistic Fluorinated Vitamin D_3 Analogs Stabilize Helix 12 of the Vitamin D Receptor

Guy Eelen,[1,5] Noelia Valle,[2,5] Yoshiteru Sato,[3] Natacha Rochel,[3] Lieve Verlinden,[1] Pierre De Clercq,[4] Dino Moras,[3] Roger Bouillon,[1] Alberto Muñoz,[2] and Annemieke Verstuyf[1,*]
[1]LEGENDO, K.U. Leuven, B-3000 Leuven, Belgium
[2]Instituto de Investigaciones Biomédicas "Alberto Sols", Consejo Superior de Investigaciones Científicas–Universidad Autónoma de Madrid, E-28029 Madrid, Spain
[3]IGBMC, Département de Biologie et de Génomique Structurales, Illkirch F-67400, France
[4]Vakgroep voor Organische Chemie, Universiteit Gent, B-9000 Gent, Belgium
[5]These authors contributed equally to this work.
*Correspondence: mieke.verstuyf@med.kuleuven.be
DOI 10.1016/j.chembiol.2008.08.008

SUMMARY

Side chain fluorination is often used to make analogs of 1,25-dihydroxyvitamin D_3 [1,25$(OH)_2D_3$] resistant to degradation by 24-hydroxylase. The fluorinated nonsteroidal analogs CD578, WU515, and WY1113 have an increased prodifferentiating action on SW480-ADH colon cancer cells, which correlated with stronger induction of vitamin D receptor (VDR)-coactivator interactions and stronger repression of β-catenin/TCF activity. Cocrystallization of analog CD578 with the zebrafish (z)VDR and an SRC-1 coactivator peptide showed that the fluorine atoms of CD578 make additional contacts with Val444 and Phe448 of activation helix 12 (H12) of the zVDR and with Leu440 of the H11-H12 loop. Consequently, the SRC-1 peptide makes more contacts with the VDR-CD578 complex than with the VDR-1,25$(OH)_2D_3$ complex. These data show that fluorination not only affects degradation of an analog but can also have direct effects on H12 stabilization.

INTRODUCTION

1,25-Dihydroxyvitamin D_3 [1,25$(OH)_2D_3$], the most active form of vitamin D_3, binds to the vitamin D receptor (VDR), a member of the nuclear receptor superfamily, which dimerizes with the retinoid X receptor (RXR). These heterodimers bind vitamin D response elements (VDREs) in target gene promoters and recruit coactivator proteins to modulate target gene transcription. 1,25$(OH)_2D_3$ is a key regulator of calcium and phosphate homeostasis and bone metabolism. In addition, 1,25$(OH)_2D_3$ has potent antiproliferative and prodifferentiating actions on various normal as well as cancerous cell types (reviewed in Dusso et al. [2005]). In the human colon cancer cell line SW480-ADH, 1,25$(OH)_2D_3$ promotes differentiation by inducing the invasion suppressor E-cadherin and by stimulating the translocation of β-catenin from the nucleus and the cytosol to the plasma membrane. In addition, ligand-bound VDR interferes with Wnt/β-catenin signaling by competing with T cell transcription factor (TCF)-4 for β-catenin binding and as such by reducing the pool of transcriptionally active TCF-4/β-catenin complexes and their target genes, such as the c-Myc oncogene (Palmer et al., 2001). The drawbacks for the use of 1,25$(OH)_2D_3$ to treat hyperproliferative disorders such as colon cancer are undesired calcemic effects. Therefore, structural analogs of 1,25$(OH)_2D_3$ have been designed to obtain a dissociation between antiproliferative/prodifferentiating action and calcemic effects. We have previously described the synthesis and the activity of the nonsteroidal analogs CD578, WU515, and WY1113 in which the complete six-membered C-ring has been deleted (Figure 1A) (Verstuyf et al., 2000; Wu et al., 2002a, 2002b) (see Supplemental Data available online for biological activity). These three analogs are fluorinated on the side chain, a modification that makes 1,25$(OH)_2D_3$ analogs more resistant to metabolic degradation by the 24-hydroxylase (CYP24) enzyme. Here we show that CD578, WU515, and WY1113 have a more potent prodifferentiating action on human SW480-ADH colon cancer cells than 1,25$(OH)_2D_3$. Behind this we found an increased VDR-based transactivating potency and a stronger induction of the interaction between VDR and coactivators SRC-1, TIF2, and DRIP205. In addition, CD578, WU515, and WY1113 are more potent than 1,25$(OH)_2D_3$ in inhibiting β-catenin transcriptional activity. Cocrystallization of analog CD578 with the zebrafish (z)VDR and an LXXLL-motif containing SRC-1 peptide revealed that the side chain fluorine atoms on analog CD578 make additional contacts with activation helix 12 (H12) of the VDR and with the loop between H11 and H12. These additional contacts stabilize the active conformation of VDR and consequently favor coactivator recruitment, which can explain the increased potency of the analog.

RESULTS AND DISCUSSION

Increased Prodifferentiating Action of Analogs CD578, WU515, and WY1113

In response to 1,25$(OH)_2D_3$, human SW480-ADH colon cancer cells underwent epithelial differentiation characterized by an increased adhesiveness and the formation of compact epithelioid cell islands. The fluorinated, nonsteroidal analogs CD578, WU515, and WY1113 induced the same morphological changes as 1,25$(OH)_2D_3$, albeit at significantly lower doses. At 10^{-9} M, there was no obvious effect of 1,25$(OH)_2D_3$, whereas a clear

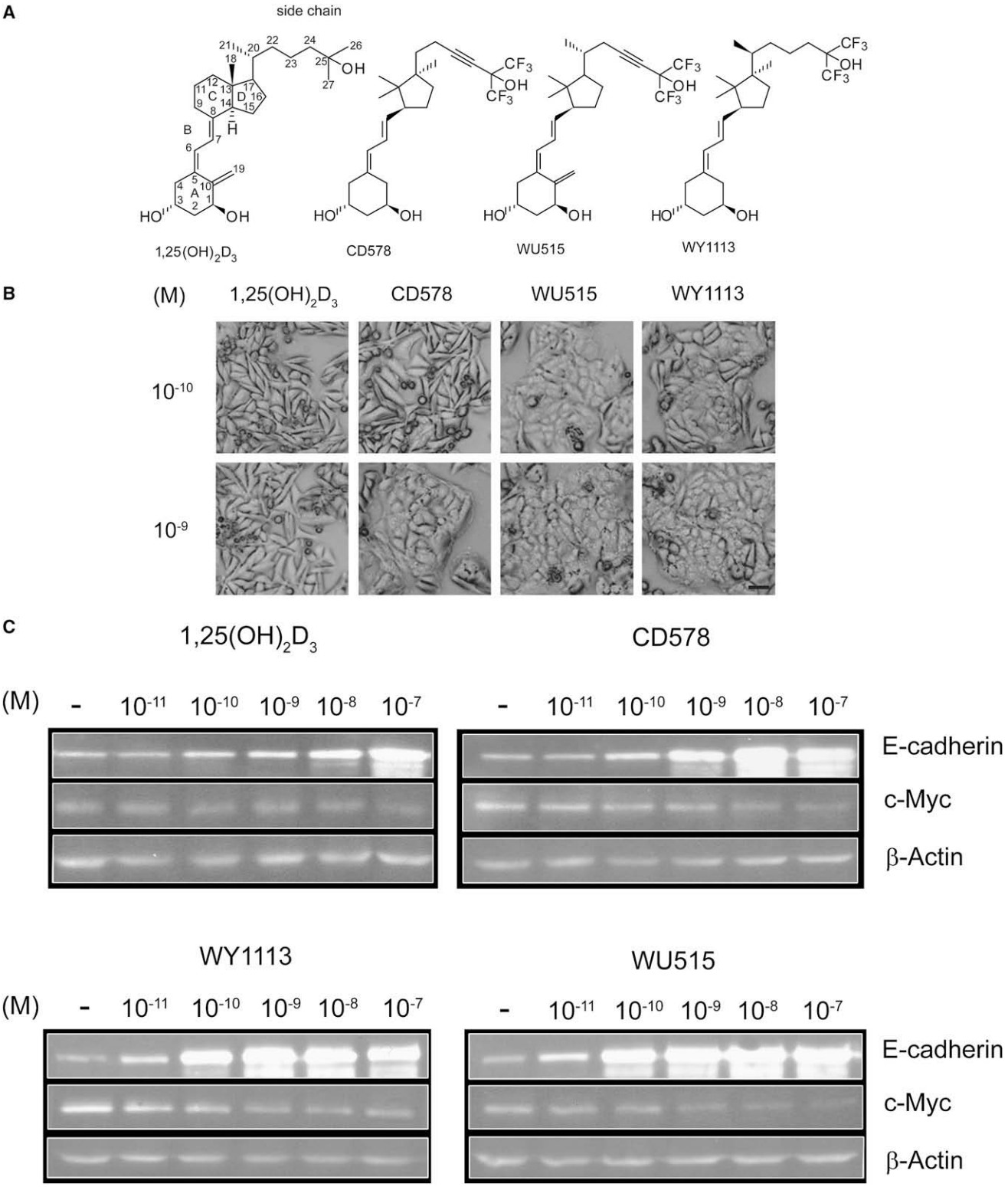

Figure 1. Chemical Structure of $1,25(OH)_2D_3$ and Analogs and their Prodifferentiating Effects on SW480-ADH Colon Cancer Cells

(A) Chemical structure of the fluorinated nonsteroidal D-ring analogs CD578, WU515, and WY1113.

(B) Differentiation of SW480-ADH cells demonstrated by phase-contrast micrographs of SW480-ADH cells treated with 10^{-10} or 10^{-9} M of each compound for 3 days. A representative experiment is shown. Scale bar = 40 μm.

(C) Western blotting analysis of the expression of E-cadherin, c-Myc, and β-actin (loading control) in SW480-ADH cells at 48 h of treatment with the indicated doses of each compound. A representative experiment is shown.

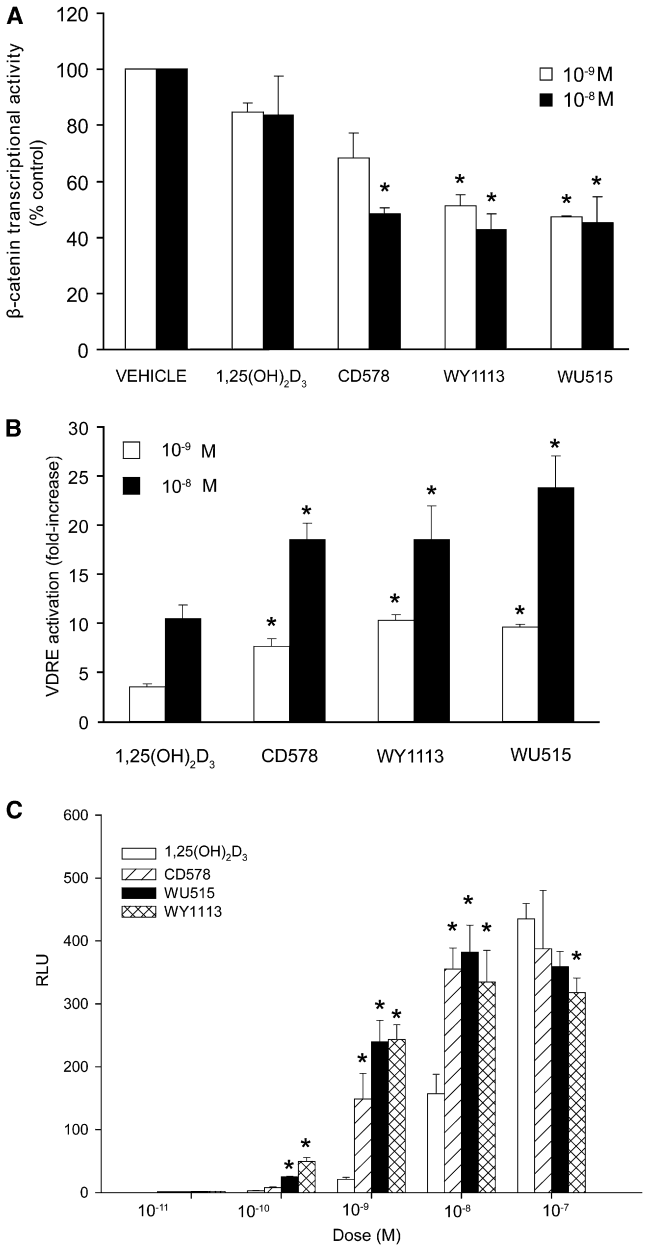

Figure 2. Effects of $1,25(OH)_2D_3$ and Analogs on β-Catenin/TCF and VDR Transcriptional Activity

(A) SW480-ADH cells were transfected with the wild-type (TOP-flash) or mutated (FOP-flash) β-catenin-TCF-responsive reporter plasmids and then treated with $1,25(OH)_2D_3$ or each analog (10^{-7} M) for 48 h. Mean values (TOP/FOP ratio, expressed as percentages of vehicle-treated cells) ± stdev obtained in three experiments using triplicates are shown. *Inhibition different from inhibition by $1,25(OH)_2D_3$ at the same dose according to Student's t test ($p < 0.05$).

(B) SW480-ADH colon cancer cells were transfected with a construct containing the *Firefly* luciferase gene under the control of four copies of a direct repeat 3 (DR3) VDRE. After 48 h incubation in the presence or absence of the indicated doses of $1,25(OH)_2D_3$ or analogs, luciferase activities were measured and normalized as described in the Supplemental Data. Bars represent fold increase ± standard deviation in normalized luciferase activity for $1,25(OH)_2D_3$- or analog-treated cells as compared with vehicle-treated cells. *Fold increase different from fold increase for $1,25(OH)_2D_3$ at the same dose according to Student's t test ($p < 0.05$). A representative experiment performed in triplicate is shown.

(C) Induction of VDR-SRC-1 interaction by transfecting human colon cancer Caco-2 cells with pVPVDR, pSG424-SRC1-NIR, pG5-LUC, and pcDNA3.1(−)/Myc-His/*lacZ* for normalization and treated with the different ligands at the indicated doses. A representative experiment of three independent experiments is shown. Data are the mean ± standard deviation of triplicate samples. *Relative luciferase units (RLU) different from RLU for $1,25(OH)_2D_3$ at the same dose according to Fisher's LSD multiple-comparison test ($\alpha = 0.05$).

morphological change was observed for CD578, WU515, and WY1113. Even at 10^{-10} M, WU515 and WY1113 had a strong prodifferentiating action (Figure 1B). The higher differentiating action of the three analogs correlated with an increased potency to induce expression of the invasion suppressor E-cadherin and a more pronounced repression of the c-Myc oncogene. When compared with $1,25(OH)_2D_3$, the dose-dependent induction of E-cadherin protein expression by CD578, WU515, and WY1113 was 100- to 1000-fold stronger (Figure 1C; see Supplemental Data for densitometric quantification). To obtain the same degree of c-Myc repression as for $1,25(OH)_2D_3$ at 10^{-8} M, 100-fold lower doses were required for CD578 and WU515. Even at 10^{-11} M, WY1113 inhibited c-Myc expression more strongly than $1,25(OH)_2D_3$ at 10^{-8} M (Figure 1C). The c-Myc oncogene is a target for β-catenin/TCF-4 at the end of the Wnt/β-catenin signaling pathway. We therefore examined the potency of $1,25(OH)_2D_3$ and the analogs to inhibit the transcriptional activity of β-catenin/TCF complexes and found that CD578, WU515, and WY1113 prevented with higher efficiency than $1,25(OH)_2D_3$ the endogenous β-catenin present in the nucleus from inducing a β-catenin/TCF-responsive reporter construct. At 10^{-9} M, the inhibition of β-catenin transcriptional activity caused by CD578, WY1113, and WU 515 was 32%, 49%, and 53%, respectively, versus 15% for $1,25(OH)_2D_3$. At 10^{-8} M, suppression of β-catenin transcriptional activity by each of the three analogs was at least 50% versus 16% for $1,25(OH)_2D_3$ (Figure 2A). Similarly, at 10^{-8} and 10^{-9} M, CD578, WU515, and WY1113 were significantly stronger (at least 1.8-fold or higher) inducers of VDR transcriptional activity than $1,25(OH)_2D_3$ (Figure 2B). The magnitude of the differences between $1,25(OH)_2D_3$ and the analogs in this last assay was more modest in comparison with the protein expression data mentioned above probably due to the different nature of the two approaches (endogenous proteins versus reporter gene assay). The increased transcriptional activity of the analogs correlated with stronger induction of VDR-coactivator interaction as was shown by mammalian two-hybrid assays with VP16-fused VDR and GAL4-DNA binding domain-fused SRC-1; tenfold lower doses of CD578, WU515, and WY1113 sufficed to obtain the same level of VDR-SRC-1 interaction induced by 10^{-7} M $1,25(OH)_2D_3$ (Figure 2C). Similar results were obtained for the interactions VDR-TIF2 and VDR-DRIP205 (see Supplemental Data). These results show that stronger biological activity of CD578, WU515, and WY1113 as compared with the natural VDR ligand is paralleled by a higher potency to induce VDR-based transactivation and to induce binding of coactivators to the VDR. It has previously been shown that biological activity highly correlates with the analog's ability to induce VDR-coactivator interactions (Yamamoto et al., 2003). This strong correlation may be partially accounted for by pharmacokinetic

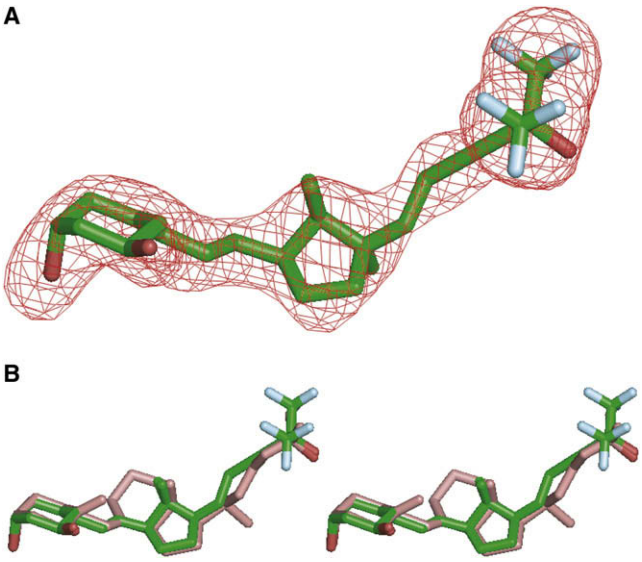

Figure 3. Conformation of the VDR-Bound CD578 Analog

(A) The analog CD578 is shown in its *Fo-Fc* electron density omit maps contoured at 3.0σ. The ligand is shown in stick representation with carbon, oxygen, and fluorine atoms in green, red, and sky blue, respectively.

(B) Stereo view of the conformation of the bound ligands. CD578 (green) and $1,25(OH)_2D_3$ (pink) are shown in stick representation after superimposed VDR complexes.

differences between analogs and $1,25(OH)_2D_3$. An issue to take into account is the increased resistance of an analog to catabolism. Some analogs are designed in such a way that they withstand 24-hydroxylase (CYP24)-mediated catabolism better than $1,25(OH)_2D_3$. CD578 and WU515 have a 23-yne structure, whereas WY1113 has a 20-*epi* configuration; two modifications that are known to result in higher resistance to CYP24-mediated degradation. Moreover, all three analogs are fluorinated at the end of the side chain. Fluorination makes the side chain less susceptible to degradation, because C-F bonds better withstand homolytic cleavage and radical oxidation (Imanishi et al., 1999). Taken together, the differences in VDR-coactivator interactions might be a mere reflection of differences in metabolism between $1,25(OH)_2D_3$ and the analogs. To exclude this possibility, 2×10^{-7} M VID400, a selective inhibitor of CYP24 (Schuster et al., 2001), was used in the mammalian two-hybrid assays with VDR and coactivators (see Supplemental Data). The addition of VID400 increased the potency of $1,25(OH)_2D_3$ to induce VDR-coactivator interaction approximately twofold. As expected, the interaction induced by CD578, WU515, and WY1113 hardly changed after addition of VID400 but remained significantly stronger in comparison with the interaction induced by $1,25(OH)_2D_3$.

Cocrystallization of the CD578-zVDR- SRC-1 Complex

To gain more insight into the molecular mechanism underlying the increased activity of the analogs, we cocrystallized CD578 together with the zebrafish (z)VDR and an SRC-1 coactivator peptide with the second LXXLL-motif containing NR box. The crystals of wild-type zVDR ligand-binding domain (LBD) bound to CD578 and SRC-1 peptide were obtained under similar conditions as for zVDR-$1,25(OH)_2D_3$ (Ciesielski et al., 2007). The zVDR LBD was used to crystallize complexes to circumvent the packing constraints of the unique crystal form obtained for the mutant human (h)VDR in which the 62 residues containing insertion region between helices H2 and H3 has been deleted (Rochel et al., 2000). We have previously shown that the structure of zVDR LBD is similar to the structure of hVDR LBD in complex with $1,25(OH)_2D_3$ (Rochel and Moras, 2006). The structure of the zVDR complex was refined at a resolution of 2.7 Å. After refinement of the protein alone, the map showed an unambiguous electron density to fit the ligand (Figure 3A). The zVDR LBD in complex with CD578 analog adopted the canonical active conformation observed for agonist-bound receptors and was similar to that of the zVDR-$1,25(OH)_2D_3$ and to the mutant hVDR-$1,25(OH)_2D_3$ complexes (Rochel and Moras, 2006). As in the zVDR-$1,25(OH)_2D_3$ complex, the insertion region between helices H2 and H3 was not visible in the electron density map, which reflects its disorder. Upon agonistic ligand binding in its LBD pocket, the VDR releases corepressors and repositions its C-terminal helix H12 in such a way that it closes off the pocket. This event favors coactivator interaction because exact positioning of H12 as a "lid" on top of the LBD pocket gives rise to a charge clamp between residues Glu446 [hGlu420] and Lys274 [hLys246] into which coactivators can dock through conserved LXXLL motifs (Vanhooke et al., 2004). In comparison to the zVDR-$1,25(OH)_2D_3$ complex, the position and conformation of the activation helix H12 in the zVDR-CD578 complex was strictly maintained. The SRC-1 peptide forms an amphipatic α-helix interacting with the hydrophobic cleft formed by H3 and H4. These interactions are similar to those described for other nuclear receptors (Darimont et al., 1998). In particular Glu446 [hGlu420] from H12 forms hydrogen bonds with the backbone amide nitrogen of Ile689 and Leu690 of the LXXLL motif. At the other end, Lys274 [hLys246] from H3 forms a hydrogen bond to the main chain oxygen of Leu694. When compared with the structure of the zVDR-$1,25(OH)_2D_3$ complex, the atomic models of zVDR bound to CD578 showed rms deviation of 0.29 Å on all Cα-atoms. The ligand was buried in the predominantly hydrophobic pocket that is conserved in all complexes. The size of CD578 ligand is 380 $Å^3$ compared with 396 $Å^3$ for $1,25(OH)_2D_3$. The volume of the ligand binding cavity is 693 and 687 $Å^3$, and CD578 and $1,25(OH)_2D_3$ occupy 54.8% and 57.6% of the pocket, respectively. The A- and secoB-rings (Figure 1A) of CD578 presented conformations similar to that of $1,25(OH)_2D_3$ (Figure 3B). The D ring of CD578 was shifted by 0.5 Å because of the modified side chain. The distance between the 1-OH and 25-OH groups varied from 16.1 Å to 15.4 Å for zVDR-CD578 and zVDR-$1,25(OH)_2D_3$, respectively. The interactions between the receptor and the ligand (79 interactions for zVDR-CD578, 71 interactions for zVDR-$1,25(OH)_2D_3$ at a distance cutoff of 4.0 Å) involved both hydrophobic and electrostatic contacts. The same conformations of the residues which form the LBD pocket were observed. The absence of the C ring in CD578 induced loss of a contact between Leu258 [hLeu230] and the atom C11 of $1,25(OH)_2D_3$ and decreased interactions with Trp314 [hTrp286] (8 interactions instead of 10 with atoms of Trp314 at a cutoff of 4 Å). Furthermore, the indole group of Trp314 [hTrp286] was shifted by 0.6 Å closer to the ligand to fill the space created by the absence of the C ring (Figure 4A). The C9 atom of CD578

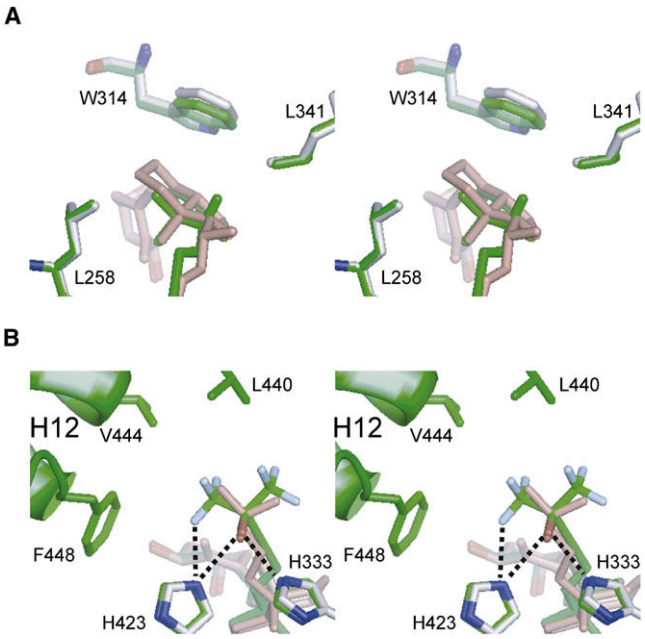

Figure 4. Close-up View of $1,25(OH)_2D_3$ and Analog CD578 in the VDR LBD Pocket

(A) Stereo views around D ring.

(B) 25-OH of CD578 (green) and $1,25(OH)_2D_3$ (pink) in the VDR LBD pocket. Carbon atoms of the residues, which are closer than 4.0 Å and important for comparison, are shown in light green and white for CD578 and $1,25(OH)_2D_3$, respectively. Nitrogen, oxygen, and fluorine atoms are shown in blue, red, and sky blue, respectively. Dotted lines represent hydrogen bonds of the CD578 complex.

Table 1. Data Collection and Refinement Statistics

Data Processing	
Resolution (Å)	50–2.7 (2.80–2.70)
Crystal space group	$P6_522$
Cell parameters (Å)	$a = b = 66.1$; $c = 265.6$
Unique reflections	10,290 (990)
Mean redundancy	17.3
R_{sym} (%)[a]	11.1 (29.9)
Completeness (%)	99.7 (100)
Mean I/σ (%)	30.3 (13.4)
Refinement	
Number of protein atoms	2010
Number of ligand atoms	33
Number of water molecules	62
Number of magnesium ion	1
RMSD bond length (Å)[b]	1.106
RMSD bond angles (°)[b]	0.006
R_{cryst} (%)[c]	22.6
R_{free} (%)[d]	28.6
Ramachandran plot (%)	
Core	90.2
Allow	9.8

Values in parentheses correspond to the highest resolution shell.

[a] $R_{sym}(I) = \Sigma_{hkl} \Sigma_i |I_{hkl,i} - \langle I_{hkl} \rangle| / \Sigma_{hkl} \Sigma_i |I_{hkl,i}|$ with $\langle I_{hkl} \rangle$ the mean intensity of the multiple $I_{hkl,i}$ observations for symmetry-related reflections.

[b] Root-mean-squared deviations (RMSD) are given from ideal values.

[c] $R_{cryst} = \Sigma_{hkl} |F_{obs} - F_{calc}| / \Sigma_{hkl} |F_{obs}|$, where F_{obs} and F_{calc} are the observed and calculated structure factor amplitudes, respectively.

[d] Calculated using a random set containing 5% of observations that were not included throughout refinement.

made a new contact with Leu341 [hLeu313] at 3.3 Å. Most interestingly, CD578 interacted through its fluorine atoms with Val444 [hVal418] and Phe448 [hPhe422] of H12 and with Leu440 [hLeu414] of the loop H11-H12 at a distance of 3.5, 3.6, and 3.3 Å, respectively. In contrast, in the zVDR-$1,25(OH)_2D_3$ complex, the ligand made no contacts with the activation helix H12 within a distance cutoff of 4.0 Å (the closest distance is 4.1 Å for Val444 [hVal418]). The canonical hydrogen bonds formed between the hydroxyl groups of the ligands and the LBD are conserved. The 25-OH group of CD578 interacted with His333 [hHis305] in the same way as the corresponding hydroxyl group of $1,25(OH)_2D_3$, whereas the hydrogen bond formed with His423 [hHis397] was weaker (3.2 Å instead of 2.8 Å) but was compensated for by an interaction again with a fluorine atom (Figure 4B). As a consequence of the stronger contacts with and the consequent stabilization of H12 in the zVDR-CD578 complex, the coactivator SRC-1 peptide made additional interactions (80 interactions with VDR in the zVDR-CD578 complex compared with 68 in the zVDR-$1,25(OH)_2D_3$ complex at a distance cutoff of 4.0 Å). Docking of WU515 and WY1113 (data not shown) indicated similar additional and stronger interactions with activation H12 of the VDR. These structural data raise the question about whether the analogs' increased potency to induce VDR/β-catenin interaction (and subsequent inhibition of β-catenin/TCF transcriptional activity) is also a consequence of H12 stabilization through the side chain fluorine atoms. A recent study hypothesized that β-catenin binding occurs at an intermediate stage between ligand-binding and the creation of the correct VDR conformation required for docking of "classical" coactivators (Shah et al., 2006). Additional modeling studies are required to determine if side chain fluorine atoms can have a stabilizing effect on this intermediate stage as well.

SIGNIFICANCE

$1,25(OH)_2D_3$ has strong antiproliferative and prodifferentiating actions on a range of cell types, including cancer cells. Actual use of $1,25(OH)_2D_3$ to treat hyperproliferative disorders is hampered by calcemic effects, hence the continuous development of chemically modified analogs of $1,25(OH)_2D_3$ with a strong dissociation between antiproliferative/prodifferentiating and calcemic actions. Side chain fluorination can increase an analog's biological activity by protecting it from metabolic degradation by the 24-hydroxylase enzyme. This study shows that the side chain fluorine atoms of the nonsteroidal $1,25(OH)_2D_3$ analogs CD578, WU515, and WY1113 contribute to the increased prodifferentiating action on colon cancer cells not only by protecting the analogs from metabolic degradation but also by increasing the stability of activation helix 12 (H12) of the vitamin D receptor through increased interactions with specific residues of H12. These

findings contribute to a better understanding of how specific chemical modifications of $1,25(OH)_2D_3$ can lead to desired biological activity and can be of great value in the development of new $1,25(OH)_2D_3$ analogs with possible therapeutic applications and—by extension—in the search for novel selective nuclear receptor modulators.

EXPERIMENTAL PROCEDURES

Reagents

$1,25(OH)_2D_3$ was obtained from J. P. van de Velde (Solvay, Weesp, The Netherlands). Synthesis of the 17-methyl-19-*nor*-21-*nor*-23-yne-26,27-F_6-$1,25(OH)_2D_3$-D-ring analog (CD578), the 23-yne-26,27-F_6-$1,25(OH)_2D_3$-D-ring analog (WU515) and the 17-methyl-19-*nor*-20-*epi*-26,27-F_6-$1,25(OH)_2D_3$-D-ring analog (WY1113) has been described previously (Verstuyf et al., 2000; Wu et al., 2002a, 2002b). The 24-hydroxylase inhibitor VID400 was obtained from A. Stütz (Novartis, Vienna, Austria).

Western Blotting

Western blotting was performed as described previously (Palmer et al., 2001). Antibodies used were mouse monoclonal anti-E-cadherin (Transduction Laboratories), mouse monoclonal anti-c-Myc, and goat polyclonal anti-β-actin (Santa Cruz Biotechnology). Blots were developed using the ECL detection system (G.E. Healthcare-Amersham).

Transactivation and Mammalian Two-Hybrid Assays

Detailed information about transactivation assays and mammalian two-hybrid assays can be found in the Supplemental Data.

Crystallography of Zebrafish (z)VDR-CD578-SRC-1 Complex

Details on expression, purification, crystallization, and subsequent X-ray crystallography, data collection and processing can be found in Table 1 and in Supplemental Data. The residue numbers in the text correspond to the zVDR sequence; the corresponding human residue numbers are given within brackets [hAAxxx].

ACCESSION NUMBERS

The PDB accession number for the coordinates of the zVDR-CD578-SRC-1 complex is 3DR1.

SUPPLEMENTAL DATA

Supplemental Data include Supplemental Experimental Procedures, Supplemental References, three figures, and one table and can be found with this article online at http://www.chembiol.org/cgi/content/full/15/10/1029/DC1/.

ACKNOWLEDGMENTS

This work was supported by grants G.0508.05 and G.0553.06 from Fonds voor Wetenschappelijk Onderzoek (FWO), NucSys (EU Marie Curie RTN), SAF2007-60341 from Ministerio de Educación y Ciencia and RTICC RD06/0020/0009 from Ministerio de Sanidad y Consumo of Spain, SPINE (QLG2-CT-220-0098) and SPINE2-complexes (LSHG-CT-2006-031220) from the European Commission and by CNRS, INSERM, ULP. G.E. is a postdoctoral researcher for FWO and N.V. is supported by RTICC RD06/0020/0009. The authors thank I. Beullens and S. Marcelis for assistance and the ESRF beamline staff (Grenoble, France) for help during data collection. The authors declare no conflict of interest.

Received: June 10, 2008
Revised: August 3, 2008
Accepted: August 6, 2008
Published: October 17, 2008

REFERENCES

Ciesielski, F., Rochel, N., and Moras, D. (2007). Adaptability of the vitamin D nuclear receptor to the synthetic ligand Gemini: remodelling the LBP with one side chain rotation. J. Steroid Biochem. Mol. Biol. *103*, 235–242.

Darimont, B.D., Wagner, R.L., Apriletti, J.W., Stallcup, M.R., Kushner, P.J., Baxter, J.D., Fletterick, R.J., and Yamamoto, K.R. (1998). Structure and specificity of nuclear receptor-coactivator interactions. Genes Dev. *12*, 3343–3356.

Dusso, A.S., Brown, A.J., and Slatopolsky, E. (2005). Vitamin D. Am. J. Physiol. Renal. Physiol. *289*, F8–F28.

Imanishi, Y., Inaba, M., Seki, H., Koyama, H., Nishizawa, Y., Morii, H., and Otani, S. (1999). Increased biological potency of hexafluorinated analogs of 1,25-dihydroxyvitamin D_3 on bovine parathyroid cells. J. Steroid Biochem. Mol. Biol. *70*, 243–248.

Palmer, H.G., Gonzalez-Sancho, J.M., Espada, J., Berciano, M.T., Puig, I., Baulida, J., Quintanilla, M., Cano, A., de Herreros, A.G., Lafarga, M., et al. (2001). Vitamin D_3 promotes the differentiation of colon carcinoma cells by the induction of E-cadherin and the inhibition of β-catenin signaling. J. Cell Biol. *154*, 369–387.

Rochel, N., and Moras, D. (2006). Ligand binding domain of vitamin D receptors. Curr. Top. Med. Chem. *6*, 1229–1241.

Rochel, N., Wurtz, J.M., Mitschler, A., Klaholz, B., and Moras, D. (2000). The crystal structure of the nuclear receptor for vitamin D bound to its natural ligand. Mol. Cell *5*, 173–179.

Schuster, I., Egger, H., Bikle, D., Herzig, G., Reddy, G.S., Stuetz, A., Stuetz, P., and Vorisek, G. (2001). Selective inhibition of vitamin D hydroxylases in human keratinocytes. Steroids *66*, 409–422.

Shah, S., Islam, M.N., Dakshanamurthy, S., Rizvi, I., Rao, M., Herrell, R., Zinser, G., Valrance, M., Aranda, A., Moras, D., et al. (2006). The molecular basis of vitamin D receptor and beta-catenin crossregulation. Mol. Cell *21*, 799–809.

Vanhooke, J.L., Benning, M.M., Bauer, C.B., Pike, J.W., and DeLuca, H.F. (2004). Molecular structure of the rat vitamin D receptor ligand binding domain complexed with 2-carbon-substituted vitamin D_3 hormone analogues and a LXXLL-containing coactivator peptide. Biochemistry *43*, 4101–4110.

Verstuyf, A., Verlinden, L., van Etten, E., Shi, L., Wu, Y., D'Halleweyn, C., Van Haver, D., Zhu, G.D., Chen, Y.J., Zhou, X., et al. (2000). Biological activity of CD-ring modified 1alpha,25-dihydroxyvitamin D analogues: C-ring and five-membered D-ring analogues. J. Bone Miner. Res. *15*, 237–252.

Wu, Y., De Clercq, P., Vandewalle, M., Bouillon, R., and Verstuyf, A. (2002a). Vitamin D_3: synthesis of seco-C-9,11-bisnor-17-methyl-1 alpha,25-dihydroxyvitamin D_3 analogues. Bioorg. Med. Chem. Lett. *12*, 1633–1636.

Wu, Y., Sabbe, K., De Clercq, P., Vandewalle, M., Bouillon, R., and Verstuyf, A. (2002b). Vitamin D_3: synthesis of seco C-9,11,21-trisnor-17-methyl-1 alpha, 25-dihydroxyvitamin D_3 analogues. Bioorg. Med. Chem. Lett. *12*, 1629–1632.

Yamamoto, H., Shevde, N.K., Warrier, A., Plum, L.A., DeLuca, H.F., and Pike, J.W. (2003). 2-Methylene-19-nor-(20S)-1,25-dihydroxyvitamin D_3 potently stimulates gene-specific DNA binding of the vitamin D receptor in osteoblasts. J. Biol. Chem. *278*, 31756–31765.

